Tribology Transactions, 49: 192-201, 2006

ISSN: 1040-2004 print / 1547-357X online
DOI: 10.1080/05698190500544668

Experimental Investigation of Thermal and Hydrodynamic Effects on Radially Grooved Thrust Washer Bearings

DOOROO KIM
George W. Woodruff School of Mechanical Engineering
Georgia Institute of Technology
Atlanta, GA 30332-0405
ROBERT L. JACKSON
Department of Mechanical Engineering
Auburn University
Auburn, AL 36849-5341
and
ITZHAK GREEN
George W. Woodruff School of Mechanical Engineering
Georgia Institute of Technology
Atlanta, GA 30332-0405

In this study, an experimental investigation on the effects of grooves on thrust washer bearings is investigated. Eight equally sized grooves are machined about 100 μm deep into one side of a flat-faced steel washer. This thrust washer bearing is located between a helical gear and its carrier and is tested on a test rig capable of measuring frictional torque and the temperature of the bearing at different speeds. It is found that the grooved washers had lower bearing temperatures and failed at significantly higher loads than the control washer with no grooves. For a test procedure with varying operating conditions, the coefficient of friction is also significantly lower for the grooved washers. However, the grooved washers had about the same coefficient of friction as the control washers at each step when the speeds are very high. The results from various tests suggest that the increased amount of lubricant passing through the grooved surface of the washer removes heat from the washer bearing by convection. This decrease in stored heat conducted from friction deters thermoelastic instabilities and the reduction of hydrodynamic stiffness due to the decrease in viscosity. Enhanced hydrodynamic load-carrying capacity is also evident in the grooved washers test results.

KEY WORDS

Bearing; Thermal Effects; Helical Gears; Wear; Friction; Washer; Grooves

Manuscript received January 31, 2005
Final manuscript approved December 21, 2005
Review led by Jane Wang

INTRODUCTION

This work investigates the effects of radial grooves on the thermal and hydrodynamic behavior of thrust washer bearings. The thrust washer bearing investigated here separates a helical planet gear from its carrier in the planetary gear-sets of automatic transmissions. This is a continuation of an experimental work (Jackson and Green *(1)*, *(2)*) and numerical analysis (Jackson *(3)*). The helical gears inherently produce an overturning moment that loads the thrust washer bearings non-axisymmetrically, and thus the friction and pressure is unevenly distributed on the washer.

It is believed that failure of the bearing is caused by thermoelastic instabilities (TEI) and thermoviscous distress (TVD) (as detailed in Jackson *(3)*). A number of past works have investigated theoretically and experimentally the mechanism of TEI in such applications as seals, clutches, and disk brakes (Anderson and Knapp *(4)*; Davis, et al. *(5)*; Decuzzi, et al. *(6)*; Dow *(7)*; Dow and Burton *(8)*, *(9)*; Banerjee and Burton *(10)*; Barber *(11)*, *(12)*; Barber and Ciavarella *(13)*; Burton, et al. *(14)*). Thrust washer bearings are very similar in geometry and function to clutches and disk brakes and are also susceptible to TEI. The event of a thermoelastic instability (TEI) results in severe distress of the thrust washer bearing and a sudden increase in temperature. This sudden increase in temperature is caused when two surfaces make contact at a point called the hot spot, and heat quickly builds up. As the temperature increases, the viscosity decreases and the surface of the hot spot bulges rapidly (see Fig. 1). Wear removes the protruding material from the hot spot, thus reducing the local temperature and decreasing TEI. However, wear can also damage the surface during distress by transferring material. After a hot spot is removed, another can develop in the same location or at a new one, thus restarting the TEI cycle. Under severe conditions, the surfaces in contact can weld together.

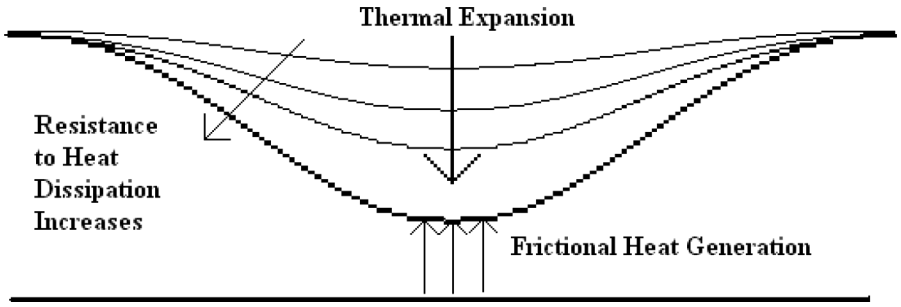

Fig. 1—Schematic of the progression of a thermoelastic instability.

Thermoviscous distress (TVD) occurs when the increasing lubricant temperature during TEI causes an increase in wear rate and a decrease in lubricant viscosity. When viscosity decreases, the hydrodynamic load-carrying capacity decreases enough such that the load is predominantly carried by asperity contact. The asperity contact causes more heat to be generated and thus the viscosity decreases even further. The two failure mechanisms of TEI and TVD can occur simultaneously, as is believed to happen in the thrust washer bearings tested in this work.

In 1949, Cope *(15)* showed that film lubrication was possible if the distance between surfaces decreased in the direction of motion (the geometric wedge) or if the density of the fluid decreased in the same direction (the thermal wedge). However, if the surfaces were close together with small variation of viscosity, the effects of the thermal wedge would outclass the geometric.

In 1960, Cameron *(16)* found that thermal distortion from the increase in temperature causes a thermal converging wedge, which was able to carry a load. In more recent studies, Kucinschi, et al. *(17)* developed a numerical model that investigated the influence of thermal deformations on radially grooved thrust washers and found that hydrodynamic lift was enhanced and that surface separation did occur in the presence of thermal deformations.

Rayleigh *(18)* originally proposed the step pattern as the simplest hydrodynamic bearing, showing theoretically that, compared to the tilting-pad, the step bearing with side leakage neglected had a considerable increase in load carrying capacity. Then Archibald *(19)* theoretically analyzed the step bearing with side leakage considered. He showed that the increase in load-carrying capacity of the step bearing is not as great as Rayleigh predicted, but still greater than that of the tilting pad, which is later experimentally proven by Kettleborough *(20)*. Thus, the step bearing grooves machined into the thrust washer bearings in this work would seem to generate higher load carrying capacities than washers without the grooves.

In 1958, Cameron and Wood *(21)* analyzed a grooved parallel surface thrust bearing assuming that the fluid takes away all the heat, and the viscosity is constant throughout the thickness of the film. In 2001, Yu and Sadeghi *(22)* numerically analyzed the effects of groove geometrical parameters to determine the optimal groove geometry for maximum load-carrying capacity. They concluded that the groove depth must be of the order of the minimum film thickness to establish hydrodynamic pressure. Furthermore, wider grooves and a higher number of grooves, up to a certain point, support more load.

The grooved or step thrust bearing is tested because the grooved pattern can easily be manufactured by chemical etching or stamping. It is also numerically determined that for an infinitely long step bearing, a greater load capacity could be reached than linear pads, but the coefficient of friction would almost be the same (Stachowaik and Batchelor *(23)*).

During the current work, the thrust washer bearing has often reached a point of distress under certain loads and speeds from what is believed to be thermoelastic instability. This point of distress is marked by a sudden increase in the COF and the bearing temperature. While the bearing is in distress, material is often transferred between bearing surfaces and/or worn away. Under severe conditions, the contacting surfaces can even weld together and cause the test rig to seize. Since this also occurs mostly at high speeds, it fits the definition of scuffing failure and wear as described in Williams *(24)*. At low speeds wear does occur, but parts rarely weld together. At low speeds the wear is abrasive (wear due to scratching with little or no surface adhesion), while at higher speeds scuffing is the primary wear mode when the bearing is under distress. Bollani *(25)* investigated the effect of lubricant additives, geometry, and speed on the occurrence of scuffing. Bollani found that scuffing is less likely to occur at low speeds, which is confirmed by the results described herein.

Salomon *(26)* provides a simplified map of fluid film failure as a function of speed and load. At low speeds, Salomon predicts that the surfaces can operate in the boundary lubrication regime without scuffing occurring. As speed is increased, the surface contact becomes more volatile and scuffing occurs in unison with surface contact. This is probably due to the increase in temperature at higher speeds causing the materials to adhere. This mode of failure is seen in the current work.

The test conditions herein, however, are slightly different than those in Jackson and Green *(1)*, *(2)*, as elaborated below. Specifically, in theory, the groove patterns would increase fluid film stiffness and load-carrying capacity, and supposedly decrease wear and the occurrence of failure. However, the step patterns in Fig. 2 are machined to about 100 μm deep into a round steel washer. This depth is significantly (orders of magnitude) larger than the depth analyzed in previous studies, and thus the hydrodynamic effect is significantly diminished. This is done by design. The deep grooves are intended to promote heat dissipation (or cooling) by allowing abundant fluid flow to pass through the interface. Note, though, that if the steps wear away (e.g., because of routine wear, debris in the oil causing abrasive wear, or intermittent contact caused by cyclic loading), the hydrodynamic lift and cooling would diminish,

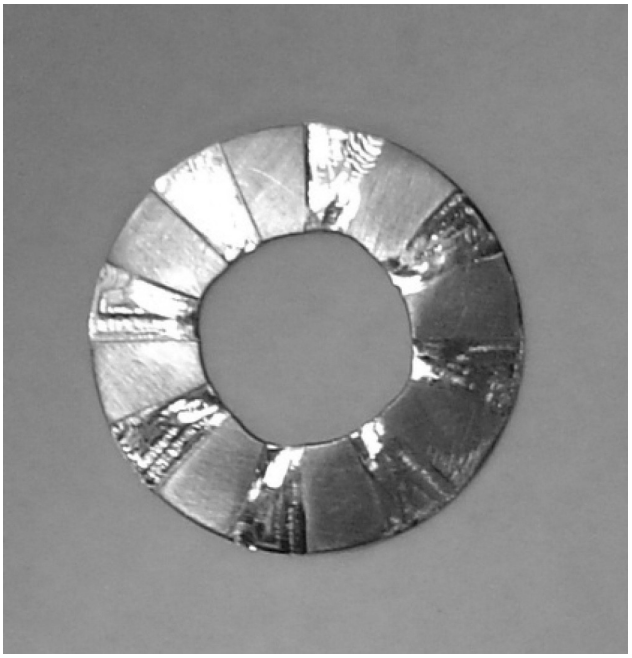

Fig. 2—Picture of step pattern in the grooved washer.

thus leading rapidly to bearing distress. It is also important to realize that one effect is entangled with the other by the thermal evolution: as the film thickness decreases, the heat increases, the viscosity decreases, etc., a cycle that is further detailed in the foregoing.

TEST RIG

The same test rig in Jackson and Green *(1)*, *(2)* is used here to test the washers allowed for controlled variation of operating conditions of the thrust washer bearings. The two varied parameters considered in this project are the axial load and the rotational speed.

An electric motor is used to drive a shaft, which drives the gears inside of the rig. The lubrication pump supplies commercial automatic transmission fluid (ATF) with a viscosity of approximately 0.06 Ns/m^2 at room temperature. A filter is used to remove any debris that might affect the performance of the washers. A lever applies axial load to the washer bearings and is attached to a pulley system where weights can be added or subtracted in order to vary the load. A schematic drawing of the test rig is shown in Fig. 3.

Thermocouples were placed in the carrier next to the thrust washer bearing to measure the bearing temperature. The thrust washer bearing, as labeled in Fig. 3, consists of both the stationary washer and test washer with the stationary washer next to the carrier. Another thermocouple is placed in a plate beneath the bearing in order to measure the temperature of the exiting lubricant. A torque sensor using strain gauges is originally implemented in the test rig. It is found, however, that the power output of the motor provides a more reliable reading. At a constant load and speed (with no acceleration), the power output of the motor is theoretically proportional to the frictional loss of the bearing. This power output is calibrated to the frictional torque and is now used to measure it. Additional information about the test rig can be found from Jackson and Green *(1), (2)*. There is one difference in the test rig, though, where in Jackson and Green *(1)*, *(2)* a slanted load applicator had been used to ensure and add to the non-axisymmetric loading. In this work, the load applicator is being replaced with an un-slanted one having parallel surfaces to facilitate more even load sharing about the washer circumference. Yet, because of the helical gears, the overturning moment is inherently present and thus the load on the washer is still not purely axisymmetric.

Commercial computer software controlled in real time the rotational speed of the electric motor. LabView^{TM}software is used to record the data acquired from the thermocouples and power output and to store the data into a text file. The computer software also is programmed to monitor the washer in real time for signs of failure. When the bearing temperature reaches 92°C, the washer is presumed failed and the motor is automatically shut down. This is done in order to prevent any damage to the test rig.

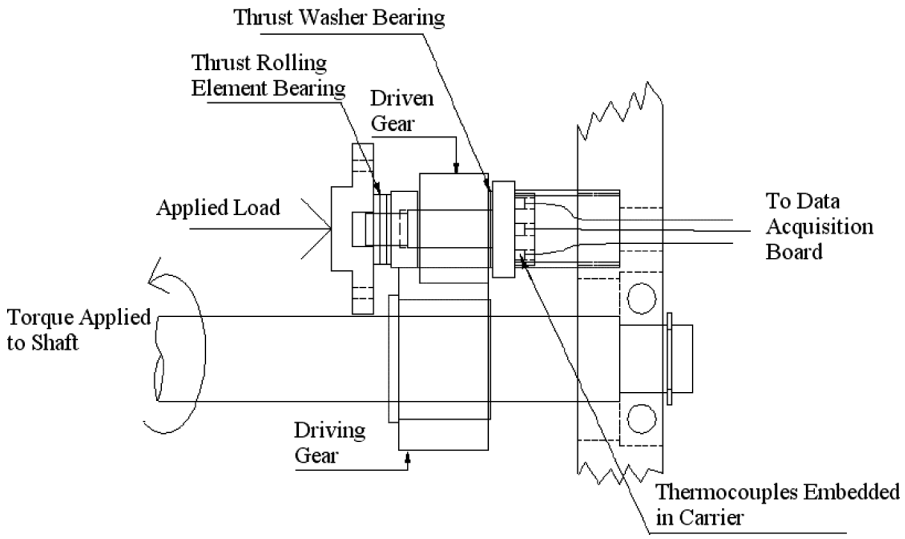

Fig. 3—Schematic drawing of the test rig.

TEST PROCEDURE

Three types of washers were tested in the current investigation. First, a flat steel thrust washer bearing is used without any grooves applied as a control. Then, thrust washer bearings that are radially grooved are tested and compared to the flat washer bearings (see Fig. 2). The groove depth is decided upon somewhat arbitrarily by the limits of onsite manufacturing capabilities. The pattern used in this experiment had eight equally sized grooves on one side of a flat-faced steel washer that has a 22.7-mm outer diameter and an 11.1-mm inner diameter. In both cases, the washer is 0.635 mm nominally thick and has an RMS roughness of approximately 0.515 μm. The grooves are milled to a depth of about 100 μm without paying special attention to the surface quality since the bottom of the milled surface is not intended to be in contact with the carrier. This depth is not optimal, as an "optimal depth" would have required an elaborate mathematical model including grooved surfaces, non-axisymmetric loading, TEI, TVD, etc. Such a model is not currently available. But even if a model had existed, the optimal value would have depended upon the objective function and operating conditions, particularly speed and load. These conditions, however, are constantly varied in the transmission and a single "optimal" value is not feasible.

The third type of washers tested were the laser surface textured (LST; see Etsion *(27)*; Brizmer, et al. *(28)*; Kovalchenko et al. *(29)*) washers in two dimples depth, shallow and deep. However, since all test results for the laser-textured and control washers are very similar practically under all testing conditions (with a slight advantage to the control washers), then for conciseness the LST test data is omitted.

For each test, a new washer and gear combination are set up within the rig, where computer software is set up to record the frictional torque and temperature of the bearing. A stationary washer is used to protect the carrier face that the thrust washer bearing is loaded against. The grooved side of the round washer is placed against the stationary washer. Once the gear and washers are set in the rig, the load is applied on the lever and the rig is closed. The appropriate test is run and the data is recorded into a text file. This data is later used to analyze the performance of each washer. Two test procedures are used for both plain and grooved washers:

1. Both rotational speed and axial load were varied simultaneously until failure is achieved.
2. The rotational speed is kept constant at the highest value, while the axial load is increased until failure is achieved.

The loads and speeds of procedure 1 are specifically designed to promote hydrodynamic lift and optimal performance of the thrust washer bearing. The test conditions are given in Table 1. Each step is run for five minutes and then the next step load and speed are changed accordingly. This procedure is run for the control, and grooved washers until the failure of the washer (i.e., the measured bearing temperature reaches 92°C). Actually, this procedure had been devised specifically to test washers that have been laser textured (Etsion *(27)*; Brizmer, et al. *(28)*; Kovalchenko, et al. *(29)*).

For the constant speed and variable load test (procedure 2), the speed is set to the highest speed (13,000 rpm) to promote hydrodynamic lift of the thrust washer bearing, although this is not necessarily the optimal condition due to temperature rise and vibrations. Each step is run for five minutes and then the load is increased according to Table 2.

Table 1—Variable Speed and Variable Load (Test Procedure 1)

Step	Desired Load	Actual Load (N)	Speed (rpm)	% Max Speed
1	10	16.32	2000	15.38
2	20	32.65	2000	15.38
3	20	48.97	3000	23.08
4	40	65.3	3000	23.08
5	60	81.62	3000	23.08
6	60	97.94	4000	30.77
7	80	114.27	4000	30.77
8	100	130.59	4000	30.77
9	130	146.92	4000	30.77
10	160	163.24	4000	30.77
11	160	179.57	5200	40.00
12	200	195.89	5200	40.00
13	250	212.21	5200	40.00
14	300	228.54	5200	40.00
15	400	244.86	5200	40.00
16	500	261.19	5200	40.00
17	600	617.76	5200	40.00
18	750	744.48	5200	40.00
19	750	744.48	6200	47.69
20	750	744.48	7200	55.38
21	750	744.48	8200	63.08
22	750	744.48	9200	70.77
23	750	744.48	10,200	78.46
24	750	744.48	11,200	86.15
25	750	744.48	12,200	93.85
26	750	744.48	13,000	100.00
27	850	855.36	5200	40.00
28	950	950.4	5200	40.00
29	1050	1045.44	5200	40.00
30	1150	1156.32	5200	40.00
31	1250	1247.4	5200	40.00
32	1350	1346.4	5200	40.00
33	1450	1453.32	5200	40.00
34	1550	1548.36	5200	40.00
35	1650	1647.36	5200	40.00
36	1730	1726.56	5200	40.00
37	750	744.48	6500	50.00
38	750	744.48	8000	61.54
39	900	855.36	8000	61.54
40	900	855.36	9500	73.08
41	1300	1298.88	9500	73.08
42	1500	1500.84	9500	73.08
43	1730	1726.56	9500	73.08
44	1730	1726.56	11,000	84.62
45	1730	1726.56	13,000	100.00

RESULTS

The data recorded is analyzed by using the Stribeck curve. In a Stribeck curve, the coefficient of friction is plotted against the product of the viscosity and bearing rotational speed divided by

TABLE 2—CONSTANT SPEED AND VARIABLE LOAD (TEST PROCEDURE 2)

Step	Actual Load (N)	Speed (rpm)	% Speed
1	32.64832	13,000	100.00
2	48.97248	13,000	100.00
3	61.2156	13,000	100.00
4	84.885632	13,000	100.00
5	97.94496	13,000	100.00
6	130.59328	13,000	100.00
7	179.56576	13,000	100.00
8	199.154752	13,000	100.00
9	261.18656	13,000	100.00
10	310.15904	13,000	100.00
11	408.104	13,000	100.00
12	506.04896	13,000	100.00
13	636.64224	13,000	100.00
14	767.23552	13,000	100.00
15	881.50464	13,000	100.00
16	979.4496	13,000	100.00
17	1077.39456	13,000	100.00
18	1191.66368	13,000	100.00

the bearing pressure. The equation form of the Stribeck curve is:

$$f = f\left(\frac{\eta V}{P}\right) \qquad [1]$$

where: f - effective coefficient of friction; η - dynamic viscosity of fluid (N s/m^2); V - rotational speed (rev/s); P - average bearing pressure (N/m^2).

A typical Stribeck curve is shown in Fig. 4. If the bearing operates on the far left side of the curve, then it experiences boundary lubrication and asperity contact. If the bearing operates on the far right side of the curve, where f is smaller, the bearing likely has a full film of lubrication separating the surfaces. Transition from mixed lubrication to full-film lubrication is marked by a "knee" at the minimum coefficient of friction.

The effective coefficient of friction is averaged for each load step. Since the torque transferred through the bearing is directly

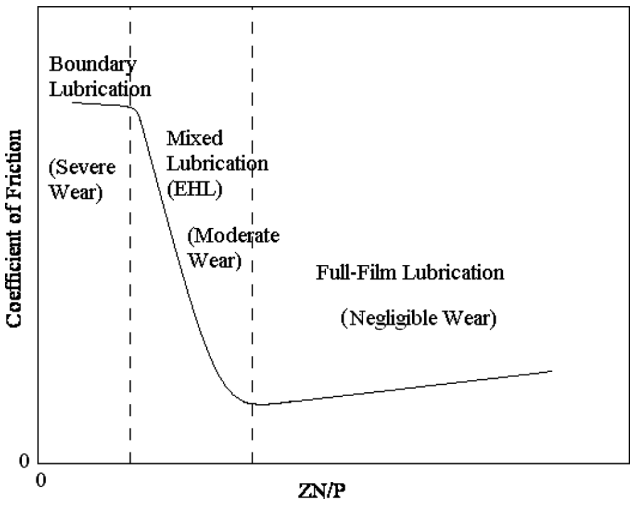

Fig. 4—Typical Stribeck curve.

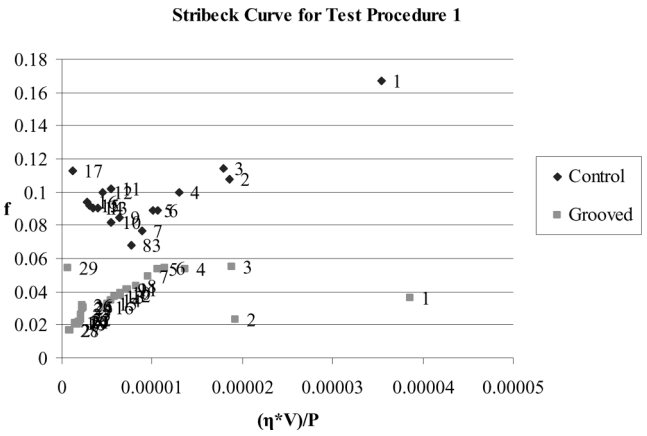

Fig. 5—Stribeck curve for test procedure 1.

related to the effective coefficient of friction, the coefficient of friction is calculated by using the torque data obtained by the power output on the test rig. This relation between the torque and the effective coefficient of friction is given by:

$$f = \frac{3}{2} \cdot \frac{T_e\left(r_o^2 - r_i^2\right)}{F_a\left(r_o^3 - r_i^3\right)} \qquad [2]$$

where: f - effective coefficient of friction; F_a - axial load (N); T_e - frictional torque (Nm); r_i - inner diameter of washer (m); r_o - outer diameter of washer (m). Equation 2 is derived in [1]. This equation assumes that the pressure distribution imposed on the washer due to asperity contact and fluid dynamics is uniform. While most likely the pressure is not uniform, Eq. [2] is still useful in providing an effective coefficient of friction which can be used to characterize bearing behavior.

Results for Test Procedure 1

Test procedure 1 is run for the control, and grooved washers. The Stribeck curves are shown for both in Fig. 5. The data collected

TABLE 3—DATA FOR CONTROL WASHER RUN IN TEST PROCEDURE 1

Step	Mean COF	Load (N)	Speed (rpm)	Lubricant Viscosity (Ns/m^2)
1	0.1670	16.32	2000	0.0564
2	0.1074	32.65	2000	0.0589
3	0.1142	48.97	3000	0.0570
4	0.0996	65.30	3000	0.0550
5	0.0889	81.62	3000	0.0532
6	0.0890	97.94	4000	0.0507
7	0.0763	114.3	4000	0.0492
8	0.0682	130.6	4000	0.0486
9	0.0845	146.9	4000	0.0459
10	0.0814	163.2	4000	0.0431
11	0.1018	179.6	5200	0.0367
12	0.0996	195.9	5200	0.0331
13	0.0906	212.2	5200	0.0311
14	0.0902	228.5	5200	0.0299
15	0.0916	244.9	5200	0.0284
16	0.0939	261.2	5200	0.0277
17-F	0.1126	617.7	5200	0.0274

Table 4—Data for Grooved Washer Run in Test Procedure 1

Step	Mean COF	Load (N)	Speed (rpm)	Lubricant Viscosity (Ns/m^2)
1	0.0358	16.32	2000	0.0613
2	0.0230	32.65	2000	0.0611
3	0.0552	48.97	3000	0.0598
4	0.0532	65.30	3000	0.0579
5	0.0536	81.62	3000	0.0565
6	0.0546	97.94	4000	0.0545
7	0.0492	114.3	4000	0.0534
8	0.0435	130.6	4000	0.0524
9	0.0408	146.9	4000	0.0517
10	0.0387	163.2	4000	0.0512
11	0.0412	179.6	5200	0.0491
12	0.0378	195.9	5200	0.0475
13	0.0366	212.2	5200	0.0469
14	0.0344	228.5	5200	0.0464
15	0.0324	244.9	5200	0.0458
16	0.0305	261.2	5200	0.0450
17	0.0217	617.8	5200	0.0427
18	0.0207	744.5	5200	0.0406
19	0.0206	744.5	6200	0.0389
20	0.0216	744.5	7200	0.0371
21	0.0216	744.5	8200	0.0353
22	0.0233	744.5	9200	0.0333
23	0.0260	744.5	10,200	0.0310
24	0.0297	744.5	11,200	0.0289
25	0.0303	744.5	12,200	0.0277
26	0.0316	744.5	13,000	0.0258
27	0.0163	855.4	5200	0.0286
28	0.0167	950.4	5200	0.0300
29-F	0.0539	1045	5200	0.0268

for the tested washers are given in Tables 3 and 4. The time of failure for the grooved thrust washer bearing is 2:21:07 and the control washer failed at step 17 after running for a time of 1:20:32. The grooved washer failed at step 29, which is 12 steps above the control washer. As seen in Fig. 5, the effective coefficient of friction for the grooved washer is consistently smaller than that for the control washer. Figure 6 shows the failed grooved washer, and although the grooves are still present, much of the virgin surface has significantly been worn off. The data and Stribeck curve generated for an additional (repeated) test are found in Table 5 and Fig. 7, respectively. The results for the second test show the same trend

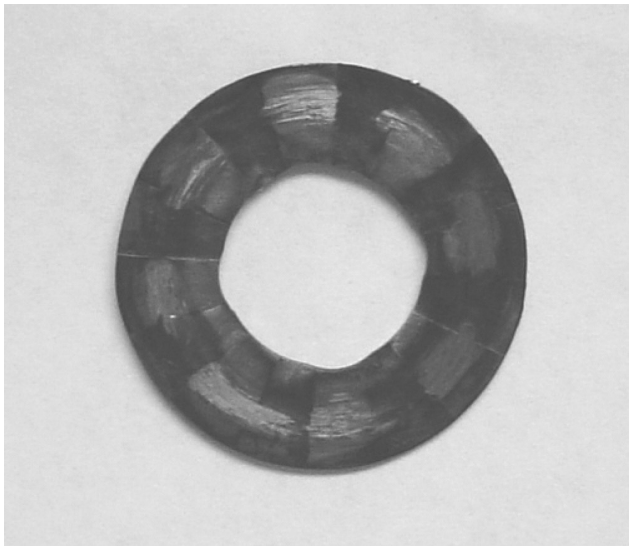

Fig. 6—Picture of worn grooved washer after run for procedure 1.

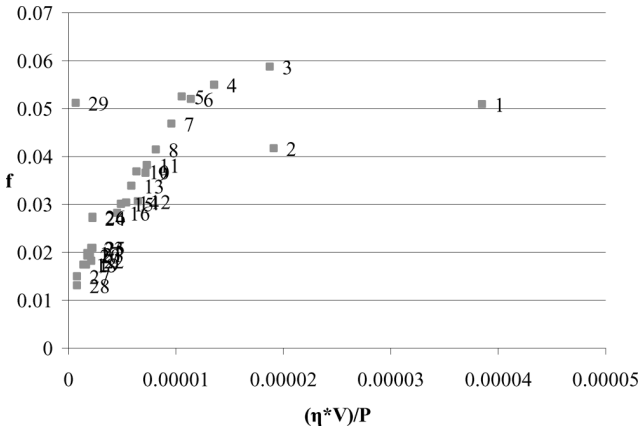

Fig. 7—Additional Stribeck curve for grooved washer in test procedure 1.

Table 5—Additional Data for Grooved Washer Run in Test Procedure 1

Step	Mean COF	Load (N)	Speed (rpm)	Lubricant Viscosity (Ns/m^2)
1	0.0507	16.32	2000	0.0599
2	0.0417	32.65	2000	0.0598
3	0.0587	48.97	3000	0.0597
4	0.0549	65.30	3000	0.0579
5	0.0523	81.62	3000	0.0567
6	0.0520	97.94	4000	0.0549
7	0.0468	114.3	4000	0.0539
8	0.0414	130.6	4000	0.0530
9	0.0365	146.9	4000	0.0530
10	0.0367	163.2	4000	0.0519
11	0.0382	179.6	5200	0.0500
12	0.0305	195.9	5200	0.0501
13	0.0338	212.2	5200	0.0479
14	0.0303	228.5	5200	0.0482
15	0.0299	244.9	5200	0.0469
16	0.0282	261.2	5200	0.0462
17	0.0198	617.8	5200	0.0439
18	0.0172	744.5	5200	0.0436
19	0.0174	744.5	6200	0.0413
20	0.0191	744.5	7200	0.0391
21	0.0195	744.5	8200	0.0371
22	0.0181	744.5	9200	0.0377
23	0.0208	744.5	10,200	0.0350
24	0.0269	744.5	11,200	0.0309
25	0.0209	744.5	12,200	0.0329
26	0.0272	744.5	13,000	0.0285
27	0.0150	855.4	5200	0.0305
28	0.0130	950.4	5200	0.0347
29-F	0.0510	1045	5200	0.0292

TABLE 6—DATA FOR CONTROL WASHER RUN IN TEST PROCEDURE 2

Step	Mean COF	Load (N)	Speed (rpm)	Lubricant Viscosity (Ns/m^2)
1	0.3633	32.65	13,000	0.0497
2	0.1635	48.97	13,000	0.0452
3	0.1329	61.22	13,000	0.0429
4	0.1099	84.89	13,000	0.0395
5	0.0937	97.94	13,000	0.0364
6	0.0716	130.6	13,000	0.0331
7	0.0531	179.6	13,000	0.0304
8	0.0501	199.2	13,000	0.0293
9	0.0513	261.2	13,000	0.0264
10-F	0.0661	310.2	13,000	0.0252

as the first test and the average COF varied by an average of 9.0% between the two tests, with a maximum difference of 45%. At failure, the COF varied by only 5.7% between the tests. The two tests also failed at precisely the same load increment, suggesting that the tests are repeatable. These relatively small variations can be attributed to manufacturing variations of the washers and slight changes in the test conditions due to wear of the test apparatus. Since washers are run to failure, damage occurs to the washers and the test apparatus, making it difficult to perform a large number of tests. However, a large number of tests were effectively run since the load and speed were incremented through a series of steps in real-time.

Since this test starts at a low rotational speed, only a small hydrodynamic lift is created between both the tested washers and the stationary washer. At low loads, this lift is still sufficient to separate the surfaces with a film of fluid. However, at some point the load overcomes the lift due to TEI and TVD. The experimental results clearly show that the addition of the grooves to the washer enhances the load carrying capacity and performance of the washer. This is deduced from Fig. 5 where the transition to hydrodynamic lubrication (i.e., the "knee" in the Stribeck curve) occurs for the grooved washer at a much smaller value of the Stribeck parameter. This happens mainly for two reasons:

(1) The increase in flow of lubricant through the grooves cools the washer and prevents TEI; and

TABLE 7—DATA FOR GROOVED WASHER RUN IN TEST PROCEDURE 2

Step	Mean COF	Load (N)	Speed (rpm)	Lubricant Viscosity (Ns/m^2)
1	0.3370	32.65	13,000	0.0388
2	0.1764	48.97	13,000	0.0354
3	0.1306	61.22	13,000	0.0338
4	0.1069	84.89	13,000	0.0324
5	0.0913	97.94	13,000	0.0312
6	0.0828	130.6	13,000	0.0300
7	0.0626	179.6	13,000	0.0286
8	0.0591	199.2	13,000	0.0277
9	0.0479	261.2	13,000	0.0268
10	0.0416	310.2	13,000	0.0260
11	0.0335	408.1	13,000	0.0253
12	0.0293	506.0	13,000	0.0245
13-F	0.0408	636.6	13,000	0.0241

TABLE 8—ADDITIONAL DATA FOR GROOVED WASHER RUN IN TEST PROCEDURE 2

Step	Mean COF	Load (N)	Speed (rpm)	Lubricant Viscosity (Ns/m^2)
1	0.3981	32.65	13,000	0.0538
2	0.2079	48.97	13,000	0.0467
3	0.1749	61.22	13,000	0.0423
4	0.1258	84.89	13,000	0.0392
5	0.0939	97.94	13,000	0.0373
6	0.0859	130.6	13,000	0.0355
7	0.0701	179.6	13,000	0.0333
8	0.0620	199.2	13,000	0.0316
9	0.0548	261.2	13,000	0.0299
10	0.0487	310.2	13,000	0.0280
11	0.0464	408.1	13,000	0.0259
12	0.0460	506.0	13,000	0.0234
13-F	0.0498	636.6	13,000	0.0225

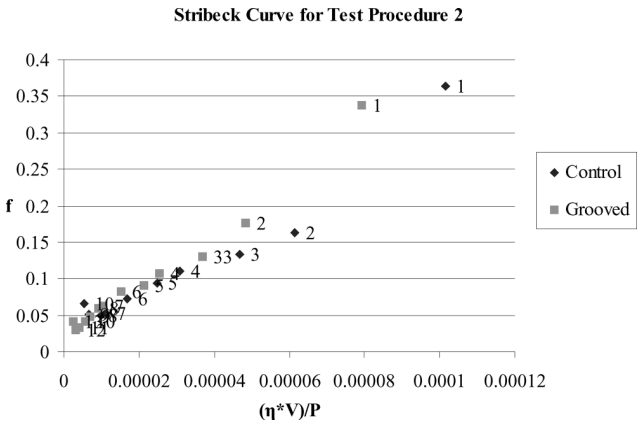

Fig. 8—Stribeck curve for test procedure 2.

Fig. 9—Picture of worn grooved washer after run for procedure 2.

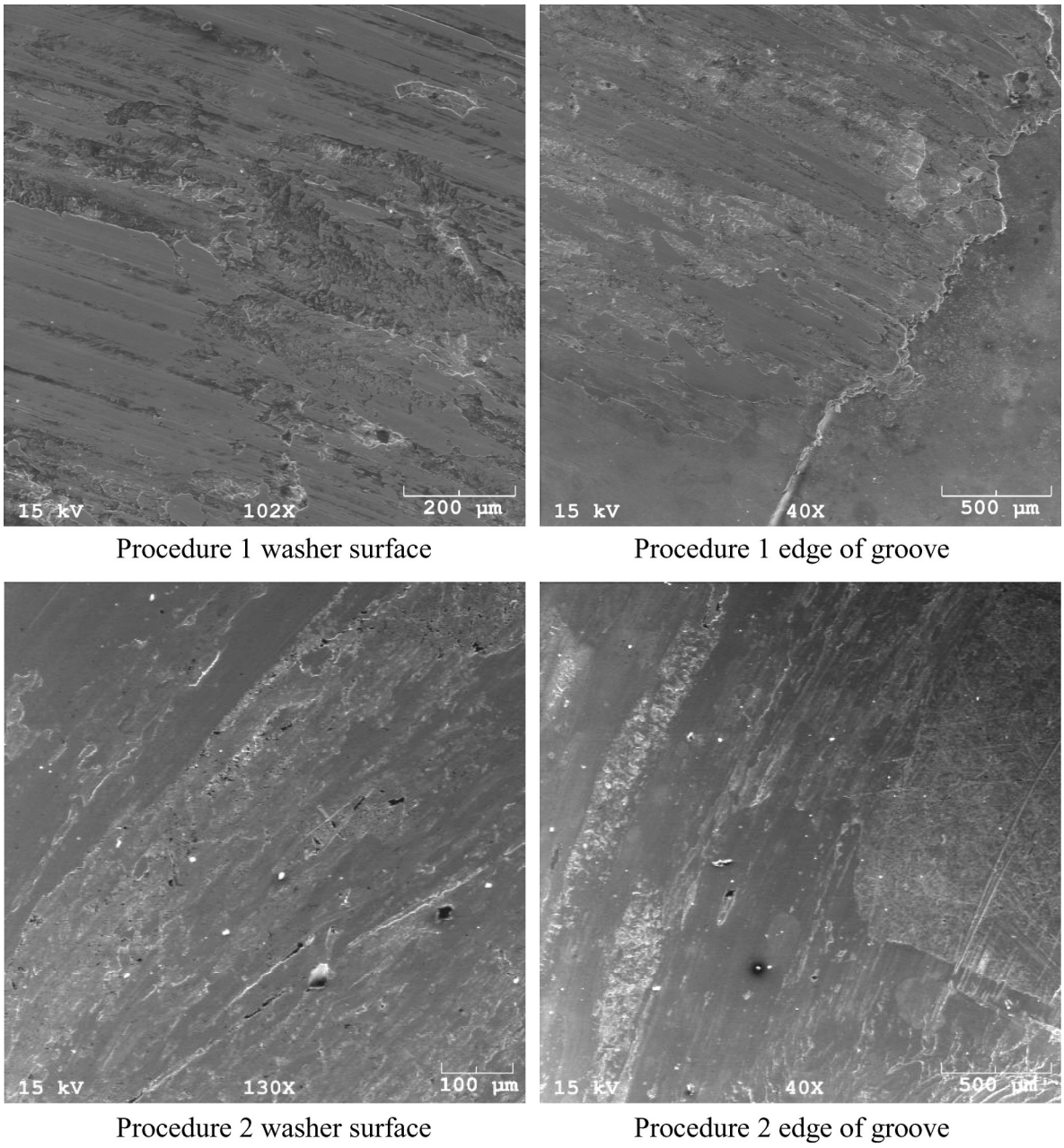

Fig. 10—SEM image of the worn thrust washer bearing surfaces.

(2) the lubricant flow over the contour of the grooves results in a "Rayleigh effect" that enhances the hydrodynamic lift.

Results for Test Procedure 2

Test procedure 2 is run for the control and grooved thrust washer bearings. The resulting Stribeck curves are shown in Fig. 8 and their respective data are given in Tables 6 and 7. The time of failure for the control washer is 45:26 at step 10 and the grooved washer failed at 1:00:51 at step 13. The effective coefficient of friction for the grooved washer is slightly larger than that of the control; however, it also failed at a load of 636.6N, which is more than twice as large as the load at step 10. The slightly higher friction coefficient may be due to the grooves causing more drag than the flat faces of the control washer while operating in or near the full film regime. It is emphasized that in this procedure the speed is kept at its highest value of 13,000 rpm, which is an extreme condition (in reality a speed such as this may occur; however, it is infrequent and its duration is short).

The grooved washer is also shown in Fig. 9 after the test is run. As expected, it appears that this washer is more severely worn than the washer tested in procedure 1 (see Fig. 6). Figure 10 shows a comparison of several SEM pictures taken of the two washer surfaces which also confirms this. The SEM images show that there is significant smearing and gouging of the washer surfaces that is typical of scuffing during TEI and TVD failure. There appear

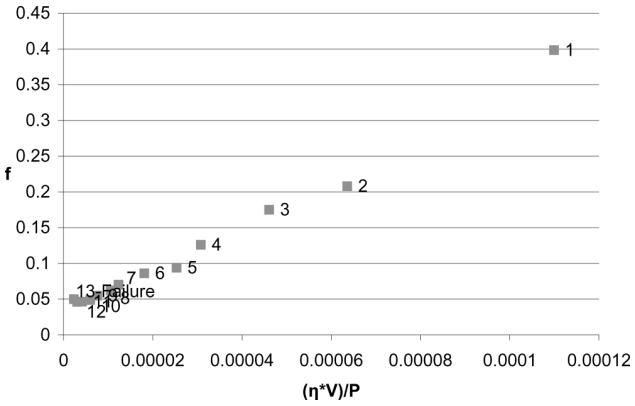

Fig. 11—Additional Stribeck curve for grooved washer in test procedure 2.

to be deeper wear grooves and gouges in the washer run under procedure 2 than procedure 1, but it is apparent that both washers failed severely. Because the washer is running at a higher speed in procedure 2 the TEI and TVD failure may have been more severe for procedure 2. The higher speeds cause higher temperature on the surfaces and thus increase the occurrence of scuffing. Still, the grooved washer failed at a higher load because the grooves allowed an increased amount of lubricant to pass along the surface of the washer. This allows the lubricant to carry heat caused by friction away by convection and the occurrences of hot spots are decreased. While thermoviscous distress (TVD) effects are larger because of the higher rotational speed, the occurrence of TEI is decreased because of the increase in lubricant flow across the surface of the washer. The data and Stribeck curve generated for an additional test are found in Table 8 and Fig. 11, respectively. The results for the second test of procedure 2 show the same trend as the first test, but by comparison it has slightly larger variations (than those reported for procedure 1 set of tests). Here, the average COF varied by an average of 15.5% between the two tests, with a maximum difference of 36.3%. At failure, the COF varied by 18.0% between the tests. The two tests also failed at precisely the same load increment, suggesting that the tests are repeatable. These relatively small variations can again be attributed to manufacturing variations and assembly of the washers in the rig and the slight changes in the test conditions due to wear of the test of apparatus.

CONCLUSIONS

The results clearly show that the grooved washers performed better than the flat-faced control washer. In every test, the coefficient of friction of the grooved washers is either similar to the other tested washers or lower. In test procedures 1 and 2, the grooved washers consistently failed much later than the control washers carrying significantly higher loads. The grooves allow more fluid to pass through the conjunction, thus cooling the temperature of the washer bearing through convection. This can decrease the effects of distress and wear from TEI and TVD by dampening the occurrence of hot spots and preventing the decrease in viscosity.

In this study, the primary effect of the deep grooves is that they enhance the flow of lubrication through the grooves and provide cooling of the surface. The grooves do provide some hydrodynamic lift; however, the deterrence of TEI and TVD has a greater impact in increasing the life of the washer.

The depth of the grooves is an important factor in both cooling the conjunction and the hydrodynamic load-carrying capacity for grooved washers. On one hand, if the groove depth is sufficiently deep it will cause an increase in the amount of side leaking that cools the conjunction. On the other hand, grooves that are too deep will have too much side flow that would decrease the hydrodynamic pressure. As explained above, the optimum groove depth needs to be found from a mathematical model that incorporates all coupled effects. Such a model may be rather complex, particularly if varying operating conditions are considered. If, in addition, wear is taken into account, i.e., the groove depth changes in time, obtaining a single "optimal groove depth" may be even more challenging. Nevertheless, the present dimensions of the grooves have proven to provide a decisive and measurable improvement, particularly as seen in the results for test procedure 1, but also in procedure 2 where the load-carrying capacity is about doubled before failure.

REFERENCES

(1) Jackson, R. L. and Green, I. (2001), "Study of the Tribological Behavior of a Thrust Washer Bearing," *Trib. Trans.*, **44**, 3, pp 504-508.

(2) Jackson, R. L. and Green, I. (2003), "Experimental Analysis of the Wear, Life and Behavior of PTFE Coated Thrust Washer Bearings Under Non-axisymmetric Loading," *Trib. Trans.*, **46**, 4, pp 600-607.

(3) Jackson. R. L. (2004), The Wear and Thermo-Elastohydrodynamic Behavior of Thrust Washer Bearings Under Non-Axisymmetric Loads, PhD Thesis, Georgia Institute of Technology, Atlanta, GA, pp 2-9.

(4) Anderson, A. E. and Knapp, R. A. (1990), "Hot Spotting in Automotive Friction Systems," *Wear*, **135**, pp 319-337.

(5) Davis, C. L., Krousgrill, C. M. and Sadeghi, F. (2002), "Effect of Temperature on Thermoelastic Instability in Thin Disks," *ASME J. Tribol.*, **124**, pp 429-437.

(6) Decuzzi, P., Ciaverella, M. and Monno, G. (2001), "Frictionally Excited Thermoelastic Instability in Multi-Disk Clotches and Brakes," *ASME J. Tribol.*, **123**, pp 865-871.

(7) Dow, T. A. (1980), "Thermoelastic Effects in a Thin Sliding Seal—A Review," *Wear*, **59**, pp 31-52.

(8) Dow, T. A. and Burton, R. A. (1972), "Thermoelastic Instability of Sliding Contact in the Absence of Wear," *Wear*, **19**, pp 315-328.

(9) Dow, T. A. and Burton, R. A. (1973), "The Role of Wear in the Initiation of Thermoelastic Instabilities of Rubbing Contact," *ASME J. Lub. Technol.*, **95**, pp 71-75.

(10) Banerjee, B. N. and Burton, R. A. (1976), "An Instability for Parallel Sliding of Solid Surfaces Separated by a Viscous Liquid Film," *ASME J. Lubr. Technol.*, **98**, pp 157-166.

(11) Barber, J. R. (1967), "The Influence of Thermal Expansion on the Friction and Wear Process," *Wear*, **10**, pp 155-159.

(12) Barber, J. R. (1969), "Thermoelastic Instabilities in the Sliding of Conforming Solids," *Proc. Roy. Soc. A.*, **312**, pp 381-394.

(13) Barber, J. R. and Ciavarella, M. (2000), "Contact Mechanics," *Int. J. Solids Struct.*, **37**, pp 29-43.

(14) Burton, R. A., Nerlikar, V. and Kilaparti, S. R., (1973), "Thermoelastic Instability in a Seal-like Configuration," *Wear*, **24**, pp 177-188.

(15) Cope, W. F. (1949), "The Hydrodynamic Theory of Film Lubrication," *Proc. Roy. Soc. A.*, **197**, pp 201.

(16) Cameron, A. (1960), "New Theory for Parallel Surface Thrust Bearing," *Engineering, London*, **190**, pp 904.

(17) Kuchinschi, B. R., DeWitt, K. J. and Pascovici, M. D., (2004), "Thermoelastohydrodynamic (TEHD) Analysis of a Grooved Thrust Washer," *ASME J. Lub. Technol.*, **126**, pp 267-274.

(18) Lord Rayleigh, (1918), "Notes on the Theory of Lubrication," *Philos. Mag.*, **35**, 1, pp 1-12.

(19) Archibald, F. R. (1950), "A Simple Hydrodynamic Thrust Bearing," *Transactions of the ASME*, **72**, pp 393-400.

(20) Kettleborough, C. F. (1955), "An Electrolytic Tank Investigation into Stepped Thrust Bearings," *Proc. Instn. Mech. Engrs.*, **169**, pp 679-688.
(21) Cameron, A. and Wood, W. L. (1958), "Parallel Surface Thrust Bearing," *ASLE Trans.*, **1**, pp 254-258.
(22) Yu, T. and Sadeghi, F. (2001), "Groove Effects on Thrust Washer Lubrication," *ASME J. Tribol.*, **123**, 1, pp 295-304.
(23) Stachowaik, G. W. and Batchelor, A. W. (1993), *Engineering Tribology*, Elsevier, Amsterdam.
(24) Williams, J. A. (1994), *Engineering Tribology*, Oxford University Press.
(25) Bollani, G. (1976), "Failure Criteria in Thin Film Lubrication with Ep Additives," *Wear*, **36**, pp 19-23.
(26) Salomon, G. (1976), "Failure Criteria in Thin Film Lubrication—The IRG Program," *Wear*, **36**, pp 1-6.
(27) Etsion, I. (2004), "State of the art in laser surface texturing." Proceedings of the 7th Biennial Conference on Engineering Systems Design and Analysis, pp 585.
(28) Brizmer, V., Kligerman, Y. and Etsion, I. (2003), "A laser surface textured parallel thrust bearing," *Trib. Trans.*, **46**, 3, pp 397.
(29) Kovalchenko, A., Ajayi, O., Erdemir, A., Fenske, G. and Etsion, I. (2004), "The effect of laser texturing of steel surfaces and speed-load parameters on the transition of lubrication regime from boundary to hydrodynamic." *Trib. Trans.*, **47**, 2, pp 593.